

Synthesis and Characterization of Cadmium Sulfide Nanoparticles by Chemical Precipitation Method

R. Aruna Devi¹, M. Latha¹, S. Velumani^{1,2,3,*}, Goldie Oza², P. Reyes-Figueroa²,
M. Rohini², I. G. Becerril-Juarez¹, Jae-Hyeong Lee⁴, and Junsin Yi^{3,*}

¹Program on Nanoscience and Nanotechnology; ²Department of Electrical Engineering (SEES), CINVESTAV-IPN, Av IPN 2508, San Pedro Zacatenco, Mexico D.F;

³School of Information and Communication Engineering; ⁴Energy and Nano Photovoltaics Lab, School of Electronic and Electrical Engineering, Sungkyunkwan University, 300, Cheoncheon-dong, Jangan-gu, Suwon, Kyeonggi-do, 440-746, South Korea

Cadmium sulfide (CdS) nanoparticles were synthesized by chemical precipitation method using cadmium chloride (CdCl₂), sodium sulfide (Na₂S) and water as a solvent by varying temperatures from 20–80 °C. The nanoparticles were characterized by X-ray diffraction (XRD), Raman spectroscopy, field emission scanning electron microscopy (FE-SEM), energy dispersive spectroscopy (EDS), High-resolution transmission electron microscopy (HR-TEM) and UV-Visible spectroscopy. XRD pattern revealed cubic crystal structure for all the synthesized CdS nanoparticles. Raman spectra showed first and second order longitudinal optical (LO) phonon vibrational modes of CdS. The size of CdS nanoparticles was found to be in the range of 15–80 nm by FE-SEM analysis, in all cases. The atomic percentage of cadmium and sulfur was confirmed to be 1:1 from EDS analysis. TEM micrograph depicts the spherical shape of the particles and the size is in the range of 15–85 nm while HR-TEM images of CdS nanoparticles exhibit well-resolved lattice fringes of the cubic structure of CdS. The optical properties of CdS were examined by UV-Visible spectroscopy which showed variation in absorption band from 460–480 nm. The band gap was calculated from the absorption edge and found to be in the range of 3.2–3.5 eV which is greater than the bulk CdS.

Keywords: Cadmium Sulfide, Chemical Precipitation, Temperature Effect, HR-TEM.

1. INTRODUCTION

In the past two decades, nanocrystalline forms of semiconductor materials and their synthesis have attracted more interest because of their unique optical and spectroscopic properties.¹ CdS nanoparticles are the most widely studied binary chalcogenide amongst II–VI semiconducting group, due to its wide energy band gap of 2.43 eV.² The various advantages of CdS as a semiconductor are availability of discrete energy levels, tunable bandgap, size dependant optical properties, good chemical stability and easy preparation techniques. The various morphologies and unique properties of CdS semiconductor intrigued researchers to exploit it in the areas of photo electrocatalysis, biotechnology and communication.³

CdS nanoparticles are ideal quantum confined semiconductors due to its optical and electronic properties.⁴ Due to wide band gap, it is used as a window material for hetero

junction solar cells to avoid the recombination of photo-generated carriers which improves solar cell efficiency.⁵ CdS is used as a *n*-type material in *p*–*n* junction solar cells along with *p*-type materials like copper indium gallium diselenide (CIGS), copper zinc tin sulfide (CZTS), gallium arsenide (GaAs), indium phosphide (InP) and cadmium telluride (CdTe).⁶ It has also extended applications in light emitting diodes,⁷ photodetectors,⁸ field effect transistors,⁹ and sensors.¹⁰ Several methods have been developed to synthesize CdS with divergent morphologies and structures such as solvothermal method,¹¹ hydrothermal method,¹² photochemical method,¹³ one pot synthesis method,¹⁴ chemical precipitation method¹⁵ etc. Among them, chemical precipitation method is a simple, clean and inexpensive technique to obtain CdS nanoparticles.³

In this report, we have employed chemical precipitation method for the preparation of CdS nanoparticles. In this work, for the first time the effect of temperature (20–80 °C) was studied on particle size, bandgap and

*Authors to whom correspondence should be addressed.

crystal structure. It is confirmed from various characterization techniques, that the temperature plays a crucial role in tuning various properties of CdS nanostructures. Thus, the future implications of such synthesized CdS nanoparticles can be its deposition as a thin film. Subsequently, such thin films can be employed as a window layer for CZTS solar cell application.

2. EXPERIMENTAL DETAILS

The chemical reagents used for nanoparticle synthesis were CdCl₂ (of 99.0% purity) Na₂S (of 98.0% purity), deionized water and absolute ethanol. All the chemicals were of pure analytical grade purchased from Sigma Aldrich, which were directly used without any further purification.

In a typical synthesis, 0.1 mole of CdCl₂ and 0.1 mole of Na₂S¹⁶ were dissolved in 25 ml of deionized water separately and continuously stirred for complete dissolution. Later, Na₂S was added dropwise into the CdCl₂ solution and the reaction was carried out by employing different temperatures (20 to 80 °C). The precursor solution gradually turned from light to dark yellow. The chemical reaction¹⁷ is as follows:



The final product was washed five times with ethanol through centrifugation process to get high purity nanoparticles. The CdS nanoparticles were collected and dried at 50 °C for 30 min and then used for characterization.

XRD patterns of CdS samples were recorded in X-ray powder diffractometer (Smartlab, Rigaku) which was operated at 45 kV and 200 mA using Cu-K α radiation ($\lambda = 1.5418 \text{ \AA}$). Micro-Raman measurements were performed using a Lab RAM Jobin Yvon spectrometer with a 632.8 nm He-Ne laser source. The morphologies of the samples were observed using FE-SEM (Auriga 3916, Carl Zeiss) and the chemical composition was measured by EDS (XFlash Detector 5010). The morphologies of the particles were confirmed by HR-TEM (JEOL, JEM-ARM200F). The optical properties were characterized using UV-Visible spectroscopy (Shimadzu Corporation UV-2401PC).

3. RESULTS AND DISCUSSION

X-ray diffraction (XRD) pattern (Fig. 1) for different temperatures were varied from 20–80 °C. It reveals cubic crystal structure for all synthesized nanoparticles with well-defined lattice planes indicating that it is nanocrystalline in nature. They are in good agreement with the hkl planes of (111), (220) and (311) which are signature markers of cubic CdS crystal (JCPDS card No: 80-0019). The average crystalline size of CdS nanoparticles were calculated using Scherrer formula,

$$D = \frac{K\lambda}{\beta \cos \theta} \quad (2)$$

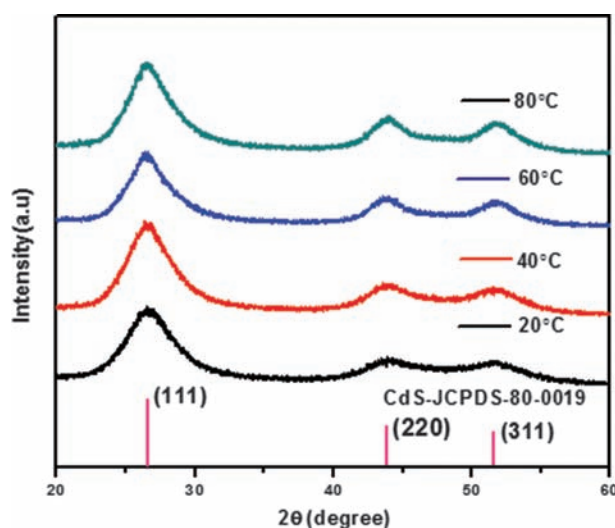


Figure 1. XRD pattern of CdS nanoparticles as a function of reaction temperature (20 °C, 40 °C, 60 °C and 80 °C).

where, D is the mean size of the ordered (crystalline) size, K is a dimensionless shape factor (0.94), λ is X-ray wavelength, β is FWHM, and θ is Bragg angle. The average crystalline size were 4.5, 5.2, 6.6 and 7 nm for 20 °C, 40 °C, 60 °C and 80 °C respectively which is in close agreement with the particle size calculated from FE-SEM

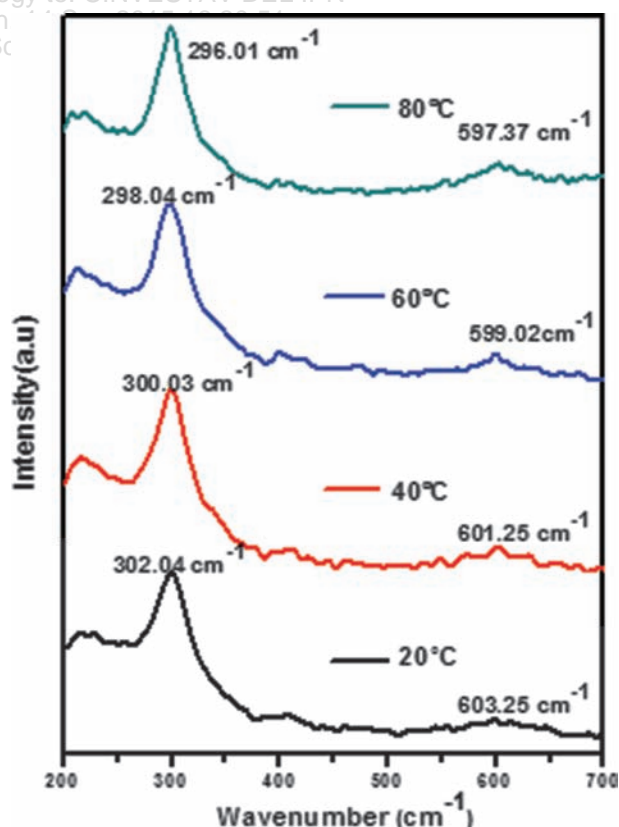


Figure 2. Raman spectra of CdS nanoparticles at different temperatures ranging from 20 °C to 80 °C.

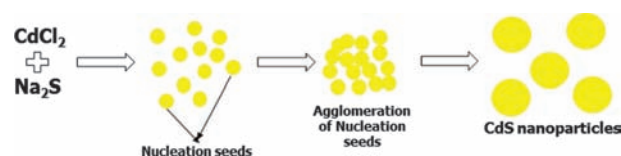
images (15 nm). Lattice parameter is calculated using the formula,

$$\frac{1}{d^2} = \frac{h^2 + k^2 + l^2}{a^2} \quad (3)$$

where, d is the atomic lattice spacing, h , k and l are miller indices, a is the lattice parameter of the crystal. When the temperature is increased, crystallinity tends to increase with decrease in lattice constant ($a = 6.29, 5.88, 5.87$ and 5.85 \AA) and increase in the particle size.¹⁸ Particle growth usually occurs via the mechanism of Ostwald ripening. Larger particles grow on account of dissolution of smaller ones. As a result, the particle size increases continuously during the growth as temperature increases.¹⁹

Raman spectra of CdS nanoparticles at different temperatures showed in Figure 2 reveals first and second order longitudinal optical (LO) phonon vibrational modes. 1LO mode appeared around 300 cm^{-1} which is the prominent peak of CdS. The 2LO mode is indicated by the raman peak at 600 cm^{-1} . We observed a small shift in raman peak towards lower wavenumber with increasing temperature.^{20,21}

FE-SEM micrographs of CdS nanoparticles showed in Figure 3 which were spherical in shape and the particle size was in the range of 15–80 nm in all cases,



Scheme 1. Growth mechanism of CdS nanoparticles.

agglomeration increases when reaction temperature is increased which is due to uncontrolled particle growth by Ostwald ripening.^{22,23} In CdS nanoparticle synthesis, majorly 2 reaction mechanisms (Scheme 1) are involved which are as follows,

1. Ostwald's ripening
2. Particle agglomeration.

Principally, the crystal growth, during *in-situ* precursor heating, follows a main path of Ostwald ripening in which the surface energy decreases when large particles are formed by employing the smaller particles. But, the ripening of nanoparticles are driven by numerous criteria like temperature of precursor, reactivity of the species etc., so that two time course growth of CdS nanoparticles were identified.

When temperature is elevated, the grain formation is fast as compared to the inferior decomposition temperature in

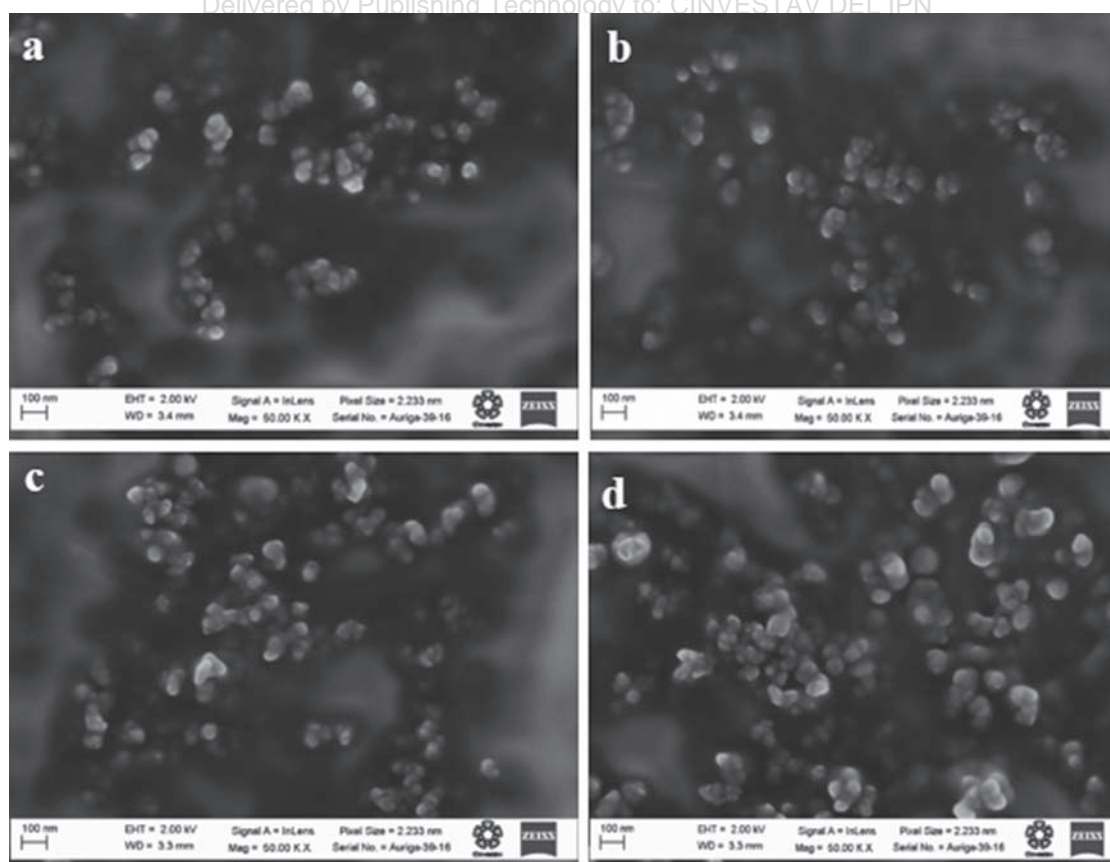


Figure 3. FE-SEM images of CdS nanoparticles (a) 20 °C (b) 40 °C (c) 60 °C and (d) 80 °C

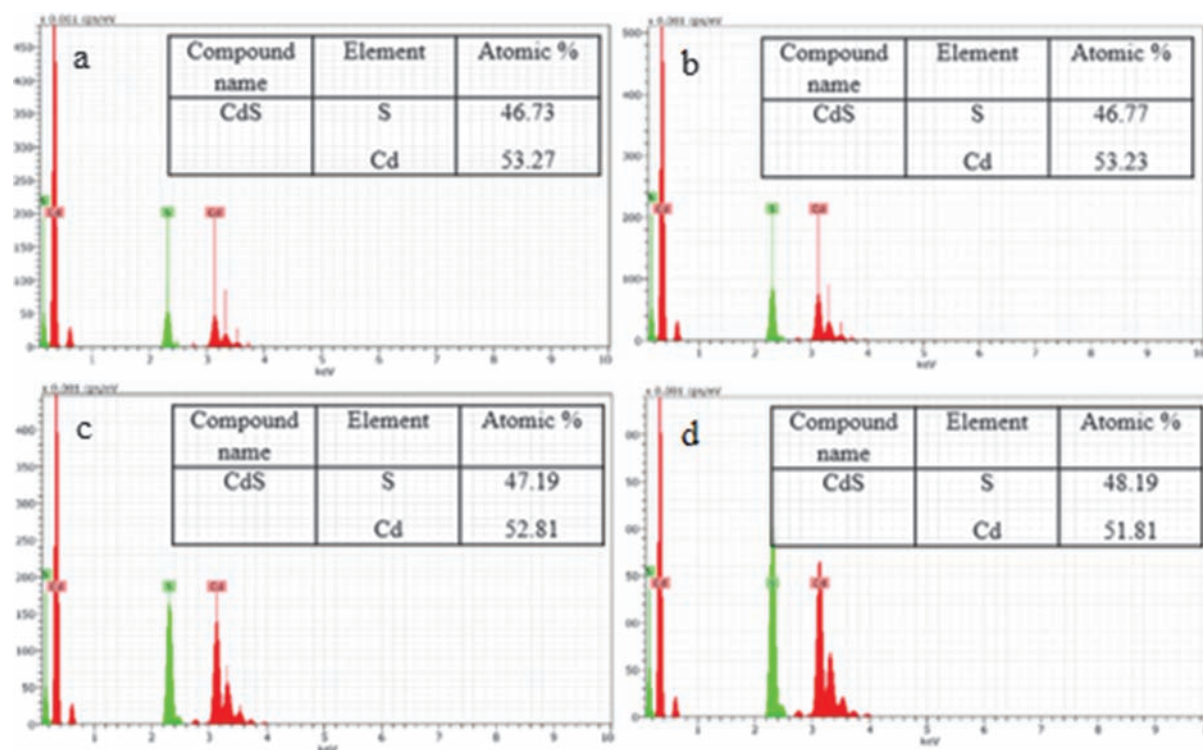


Figure 4. EDS spectrum of CdS nanoparticles (a) 20 °C, (b) 40 °C, (c) 60 °C and (d) 80 °C.

which the nuclei formation rate is absolutely slower. Moreover, the matrix will act as a reaction chamber in which the crystal can only grow to a certain size, preventing the coalescence of nanoparticles. Consecutively, the polymer chain removal will promote coalescence of particles and also the agglomeration of the previously building units.²⁴ EDS analysis (Fig. 4) confirmed the stoichiometric ratio of 1:1 for Cd and S. As temperature increases S:Cd increases since surface to volume ratio decreases with increasing cluster size.²³

Nanosized spherical particles were observed using TEM (Fig. 5) which is due to the free surface area and surface energy reductions. Because, the growth and nucleation of CdS nanoparticles from reaction solution is principally governed by the competition between surface and volume free energies of the particle. This can be achieved by adopting a crystal structure amenable to the formation of a sphere like nucleus by exposing close-packed low-energy planes as facets on the surface of the nucleus.²⁵ As temperature increases, particle size is increased due to Ostwald ripening, the smaller particles are merged into larger ones. We observed this increase up to the range of 85 nm when the temperature is reached to 80 °C. HR-TEM images (Fig. 6) of CdS nanoparticles for different temperatures exhibit well resolved lattice fringes with the interplanar spacing of 0.33 nm (20 °C), 0.32 nm (40 °C), 0.31 nm (60 °C) and 0.30 nm (80 °C) assigned to (111) plane of the cubic CdS structure.

UV-Visible absorbance spectrum are shown in Figure 7. The absorption peak shows blue shift in relation to the bulk CdS (512 nm) which is due to increased binding energy of the exciton.²⁶ The optical absorption edge in the blue shift indicates the formation of CdS particles in the nanometer regime. As temperature increases, wavelength is shifted to higher wavelengths. Thus, the wavelength is increased

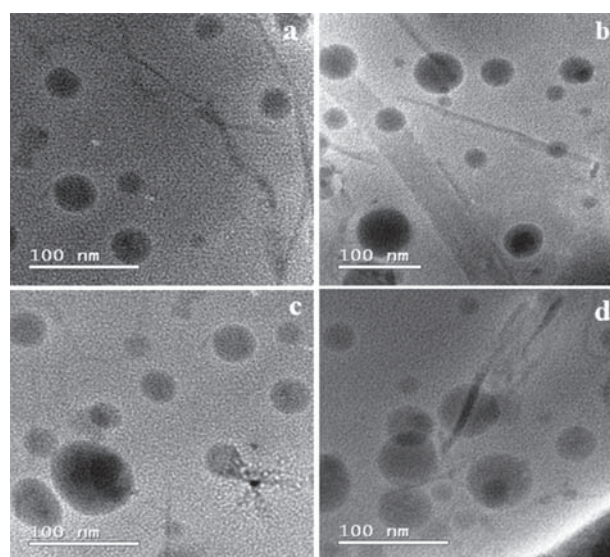


Figure 5. TEM images of CdS nanoparticles (a) 20 °C, (b) 40 °C, (c) 60 °C and (d) 80 °C.

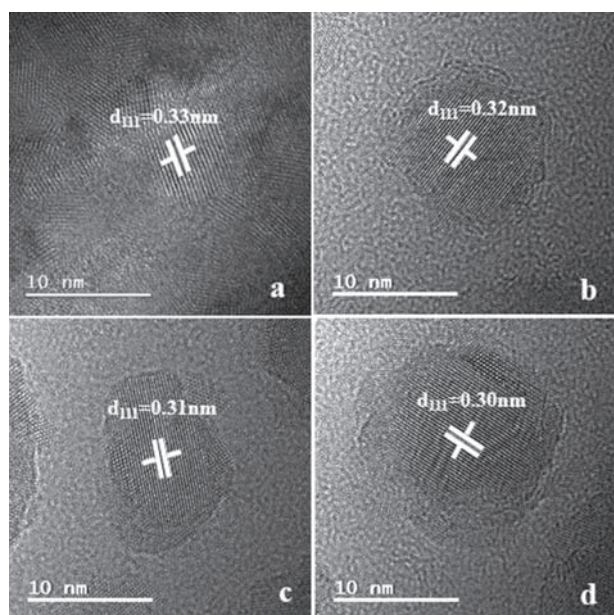


Figure 6. HR-TEM images of CdS nanoparticles (a) 20 °C, (b) 40 °C, (c) 60 °C and (d) 80 °C.

from 460 to 480 nm and the bandgap (inset) was found to be in the range of 3.5 to 3.2 eV. Size of the particles is directly related to the absorption wavelength, Ostwald ripening is observed as a continuous shift of the excitonic absorption band to longer wavelengths.²³ As temperature increases, bandgap is decreased with the increase in particle size. This is because at high reaction temperatures, the rate of particle growth is much higher for the primary units to stack in a smooth and gentle manner, whereas when the temperature decreases, the primary unit stacking is continuous and slow.

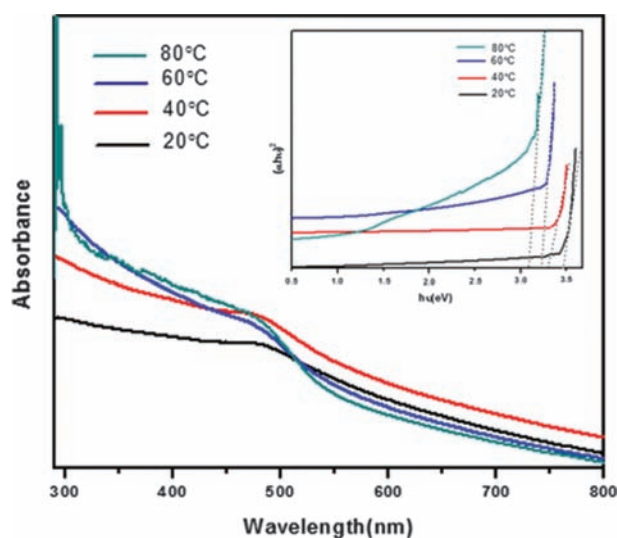


Figure 7. UV-visible absorption spectra of the CdS nanoparticles synthesized at different reaction temperature and the inset shows the $(\alpha h\nu)^2$ versus $h\nu$ plots with corresponding fitting of the samples.

4. CONCLUSIONS

In the present work, CdS nanoparticles were synthesized using chemical precipitation method by varying temperatures from 20 to 80 °C. Temperature plays a vital role in synthesizing CdS nanoparticles, which affects the particle size, bandgap and morphology. Cubic crystal structure was observed in all cases and crystallinity increased as temperature increases. As temperature increases, both particle size as well as agglomerations increased due to Ostwald ripening. Spherical nanoparticles were observed because surface to volume ratio decreases. Bandgap is reduced as temperature increases, which is in good agreement with the particle size because, increased particle size leads to decrement in the bandgap. Thus, the synthesized CdS nanoparticles will be deposition as a thin film and it can be used as a window layer for solar cell applications.

Acknowledgments: The authors would like to thank CONACyT for their financial support through project no: 326/11. We also thank Marcela Guerrero (X-ray diffraction), J. E. Remero Ibarra (FE-SEM) and Alvaro Pascual (HR-TEM) for characterization help. We thank the partial financial support from the projects CeMIE-Sol 207450/P26 and from Human Resources Development Program grant (No. 20124010203280) of the Korea Institute of Energy Technology Evaluation and Planning (KETEP) funded by the Ministry of Trade, Industry and Energy of the Korean government. One of the authors (S. Velumani) is thankful for the support from MSIP (Ministry of Science, Ict & future Planning). (141S-6-3-0641), South Korea.

References and Notes

- G. Z. Wang, W. Chen, C. H. Liang, Y. W. Wang, G. W. Meng, and L. D. Zhang, *Inorganic Chemistry Communications* 4, 208 (2001).
- A. Mercy, K. S. Murugesan, B. M. Boaz, A. J. Anandhi, and R. Kanagadurai, *Journal of Alloys and Compounds* 554, 189 (2013).
- A. Mercy, R. S. Selvaraj, B. M. Boaz, A. J. Anandhi, and R. Kanagadurai, *Indian Journal of Pure Applied Physics* 51, 448 (2013).
- Y. Cao, P. Hu, and D. Jia, *Applied Surface Science* 265, 771 (2013).
- V. Singh, P. K. Sharma, and P. Chauhan, *Material Characterization* 62, 43 (2011).
- Y. Kashiwaba, K. Isojima, and K. Ohta, *Solar Energy Materials & Solar Cells* 75, 253 (2003).
- Y. Wang, S. Ramanathan, Q. Fan, F. Yan, Morkoc, and H. Bandyopadhyay, *J. Nanosci. Nanotechnol.* 6, 2077 (2006).
- R. M. Ma, L. Dai, and G. G. Qin, *Nano Lett.* 7, 868 (2007).
- X. Duan, Y. Huang, R. Agrawal, and M. C. Lieber, *Nature* 421, 241 (2003).
- T. Fu, *Mater. Res. Bull.* 48, 1784 (2013).
- A. Phuruangrat, T. Thongtem, and S. Thongtem, *J. Exp. Nanosci.* 4, 47 (2009).
- Z. Jinxin, Z. Gaoling, and H. Gaorong, *Chem. Chin.* 2, 98 (2007).
- M. Marandi, N. Taghavinia, A. Iraj, and S. M. Mahadavi, *Nanotechnology* 16, 334 (2005).
- H. Tong and Y. J. Zhu, *Nanotechnology* 17, 845 (2006).
- V. Singh and P. Chauhan, *J. Phys. Chem. Solids* 70, 1074 (2009).
- V. Singh and P. Chauhan, *Chalcogenide Letters* 6, 421 (2009).

17. J. Barman, J. P. Borah, and K. C. Sarma, *Chalcogenide Letters* 5, 265 (2008).
18. S. Kumar, A. K. Chawla, N. Kumar, and R. Chandra, *RSC Advances* 1, 1078 (2011).
19. M. Z. Iqbal, S. Ali, and M. A. Mirza, *Coden Insmac* 48, 51 (2008).
20. R. R. Prabhu and M. A. Khadar, *Bull. Mater. Sci.* 31, 511 (2008).
21. Z. Dai, J. Zhang, J. Bao, X. Huang, and X. Mo, *Journal of Materials Chemistry* 17, 1087 (2007).
22. K. Manzoor, S. R. Vadera, N. Kumar, and T. R. N. Kutty, *Solid State Communication* 129, 469 (2004).
23. T. Vossmeier, L. Katsikas, M. Gienig, I. G. Popovic, K. Diesner, A. Chemseddine, A. Eychmiiller, and H. Weller, *J. Phys. Chem* 98, 7665 (1994).
24. H. C. Warad, S. C. Ghosh, B. Hemtanon, C. Thanachayanont, and J. Dutta, *Science and Technology of Advanced Materials* 6, 296 (2005).
25. R. Banerjee, R. Jayakrishnan, and P. Ayyub, *J. Phys: Condens. Matter* 12, 10647 (2000).
26. T. Shanmugapriya, R. Vinayakan, K. George Thomas, and P. Ramamurthy, *Cryst. Eng. Comm.* 13, 2340 (2011).

Received: 17 August 2014. Accepted: 5 March 2015.

Delivered by Publishing Technology to: CINVESTAV DEL IPN
IP: 148.247.99.101 On: Mon, 14 Sep 2015 16:30:51
Copyright: American Scientific Publishers